JOURNAL OF ATMOSPHERIC AND OCEANIC TECHNOLOGY

A report on progress on Corrected Moments in Antenna Coordinates 2.0

SCOTT COLLIS* AND JONATHAN HELMUS

Environmental Science Division, Argonne National Laboratory

ABSTRACT

In 2010 the Atmospheric Radiation Measurement program procured a number of 3 and 5cm wavelength radars for documenting the macrophysical, microphysical and dynamical structure of precipitating systems. In order to maximize the scientific impact the program supported the development of an application chain to correct for various phenomena in order to retrieve the "point" values of moments of the radar spectrum and polarimetric measurements. This report details the motivation, science and progress to date as well as charting a path forward.

1. Introduction

The Atmospheric Radiation Measurement Program (Mather and Voyles (2012)) (ARM) has a long history of sensing clouds in the column using the Millimeter Cloud Radar (MMCR, Now Ka-Band Zenith Radar or KaZR). Starting in 2010 ARM embarked on program to better characterize the domain surrounding the column using scanning radars at millimeter and centimeter wavelengths. Processing for the shorter wavelengths has been previously published Kollias et al. (2013) this report is limited to 5 and 3cm wavelengths. Due to the agility and lower cost per radar the program opted not to operate the common wavelength of 10cm (S-Band) which is robust to liquid water path attenuation in all but the most severe storms. This necessitates the development of robust code for the correction of issues due to the two way propagation of the radar through medium that both scatters and attenuates. In addition, the trade off between wavelength, maximum unambiguous range and Doppler nyquist velocity means the radars alias at 12.4 and 16.52 ms^{-1} for 3 and 5cm respectively when operating in a baseline mode (such as during the Mid-Latitude Convective Continental Clouds Experiment $\mathrm{MC}^3\mathrm{E}$ (Jensen et al. (2015)). Due to extreme velocities of scatterers aloft and, in places such as Oklahoma, at the surface, aliasing is common and requires post moment calculation dealiasing. There are many techniques for dealiasing Doppler velocities (eg James and Houze (2001)) however on testing we found these techniques to be either difficult to implement in an operational chain or lacking in robustness.

*Corresponding author address: Scott Collis, Argonne National Laboratory, Environmental Science division, 9700 South Cass Ave, Argonne, IL 60514
E-mail: scollis@anl.gov

When we first attempted to build a processing chain each step made its own decision on where to conditionally run based on various measurements of "quality" such as the co-polar (zero lag) correlation coefficient ρ_{HV} and Normalized Coherent Power (NCP, also referred to as Signal Quality Index or SQI). These are defined as:

$$\rho_{HV}(0) = \frac{|<S_{VV}S_{hh}^{*}>|}{\sqrt{<|S_{HH}|^2><|S_{VV}|^2>}} \tag{1}$$

$$NCP = \frac{P_{coh}}{P_{DC}}. \tag{2}$$

Where the S terms are elements of the scattering matrix, P_{coh} is the coherent part of the doppler spectrum and P_{DC} is the incoherent part. Since ARM radars use magnetron transmitters the phase is randomized from pulse to pulse so when a first trip return is mixed with a return from a scatterer beyond the maximum unambiguous range the derived radar Doppler spectrum when averaged over many pulses is flat and the NCP is low. While the Doppler spectrum from a first trip has structure from which (depending on the method) a peak can be found and Doppler velocity determined and the NCP approaches 1.0. However, the usefulness of NCP alone in second trip detection breaks down in regions of high spectral width. When the spectral width approaches the nyquist velocity, even in areas of purely first trip, the NCP decreases. This is especially troublesome in regions of high convergence and divergence in convective storms, often causing false flagging of these regions.

To overcome the issues of arbitrary decision making and faults in using NCP alone to detect multiple trips our application chain, Corrected Moments in Antenna Coordinates first attempts to identify the nature of the scattering medium at the gate. This gate-ID is performed before any corrections are applied so it is different to hydrometeor identification codes (eg Dolan and Rutledge (2009), Wen et al. (2015), Al-Sakka et al. (2013) etc.) that seek to gain microphysical insight. Gate-ID is performed for the purpose of objectively determining where future algorithms should be applied. Since we are implementing CMAC2.0 using the Python-ARM Radar Toolkit (Py-ART, Heistermann et al. (2014)) we can use the the identifications to construct a gate filter.

2. Application chain

There exists many algorithms in the scientific literature for the quality control and correction of radar data. Far to many to adequately asses and implement. However, given Py-ART's data model driven approach it is possible to design an application chain that is highly modular and task based. Each component has a particular job and can be replaced as better algorithms are published (and, ideally, code shared). As stated in the previous section, the overarching idea behind CMAC2.0 is a gate-ID is created and determines the conditional application of algorithms. At the time of writing implemented classes are: Rain, melting layer, ice, second trip and no significant scatterer. Dealiasing, for example would run on the set of all classes except "no significant return" while retrievals of specific attenuation would run on the class of "rain". This approach requires that the gate-ID is run on the pre-corrected data. However, as discussed in sec 1, radar provided measurements alone are not sufficient to constrain the problem of gate-ID, especially the identification of multiple trips. There are a number of pre-ID retrievals and inputs we can generate to constrain the problem, however, and these are described in a.

The Application chain for CMAC2.0 is shown in fig 1 and can be broken down to:

- Pre-ID calculations of texture and mapping sounding data to radar gates
- Ascribing membership functions to gate classes, scoring of gates and classification at the gate of predominate scatterer.
- Dealiasing of Doppler velocities.
- Extraction of propagation differential polarimetric phase from instrument measured differential polarimetric phase.
- Calculation of specific differential phase.
- Calculation of specific attenuation.
- Integrate and apply to reflectivity.
- Calculate rain rate for liquid precipitation using specific attenuation.

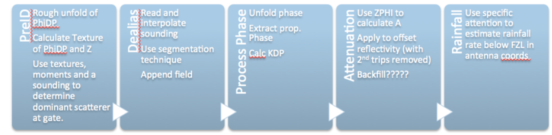

FIG. 1: The Application chain for Corrections in Antenna Coordinates 2.0

a. *Calculations performed to aid identification of scatterers at gate*

There are two steps to add information in order to determine dominant scattering process at the gate: Mapping temperature to gate locations and using texture of radial velocity as a discriminant of significant scattering.

Since Py-ART already ascribes a cartesian displacement from the radar for each gate using a simple $\frac{4}{3}R_e$ standard atmosphere propagation model CMAC2.0 simply interpolates sonde data available from ARM soundings (via the interpolated sonde product DOI).

The idea behind texture is that when second trips (or no-trips) dominate, due to the pulse-to-pulse randomized phase of a magnetron transmitter, radial velocity should vary, from gate to gate, between nyquist and negative nyquist randomly. As long as there is some structure to the radar Doppler spectrum the signal processor should be able to pick a peak and determine the 1st moment being the radial velocity. Thus the gate-to-gate and azimuth to azimuth variation, or texture of Doppler velocity should be able to act as a good discriminant of significant returns. The abstract concept is for a central pixel, (i,j) in 4, the points surrounding in a n by m kernel are collected then the statistic (eg variance) is calculated on the set of points and is returned as the (i,j)th value in the resultant 2D (range, time/azimuth) array.

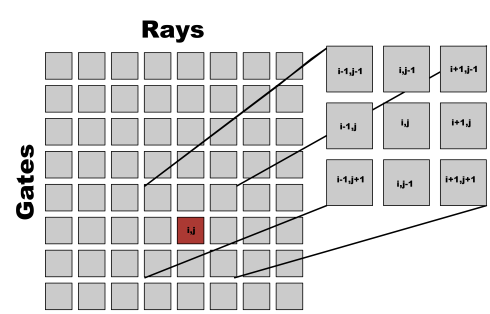

FIG. 2: Illustration of the concept of a moving filter over range gates of adjacent rays. The center element, (i,j) is calculated by passing surrounding elements. The footprint of the surrounding elements is determined by the kernel. In many cases we use a 3x3 kernel

The challenge comes from the desire to calculate this pre-correction. Doppler folding will generate a significant signal in the texture field if done purely on radial velocity values. However projection of radial velocity values onto a unit circle allows a smooth transition from positive nyquist to negative nyquist and there is a branch of mathematics dealing with the statistics of directions and magnitudes known as directional statistics (Wikipedia (2016)). Values from positive nyquist to negative nyquist are projected onto a circle with $\theta = 0$ to π and the standard deviation is given by:

$$x = \cos\theta \tag{3}$$
$$y = \sin\theta \tag{4}$$
$$R = \sqrt{\bar{x}^2 + \bar{y}^2} \tag{5}$$
$$S = \sqrt{-2 * \log R} \tag{6}$$

Figure 3a shows a typical radial velocity field, with folds, from the ARM C-SAPR at the Southern Great Plains. Figure 3b shows the texture field calculated by passing eq. 6 over data in 3a using a 3x3 kernel as shown in fig 4.

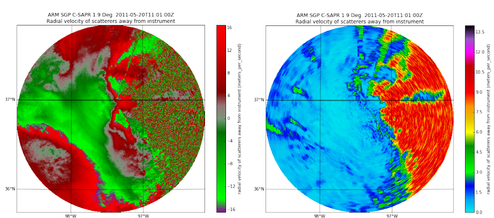

(a) Radial velocity (b) Texture

FIG. 3: Calculations of texture of radial velocity from the C-Band Scanning ARM Precipitation Radar (C-SAPR) using circular statistic to avoid false texture on folds

There are clearly higher values of texture where there are no significant returns while texture falls quickly over the precipitation echo boundaries. However the exact values of texture to be used in the membership function to delineate between significant and non-significant will depend on many factors that influence texture including number of samples, signal to noise etcetera. Plotting a histogram of texture values yields two distinctly separated populations of gates. To find the discrimination point we use Scientific Python's (Jones et al. (2001–)) continuous wavelet transform-based peak finding algorithm (Du et al. (2006)) to find the location of the left and right peak. The cut off is then decided by finding the minimum value, or valley, between the two peaks. Ad-hoc testing shows this to be robust even when changing radar types. We tested with X,C and Ka band radars all using different configurations.

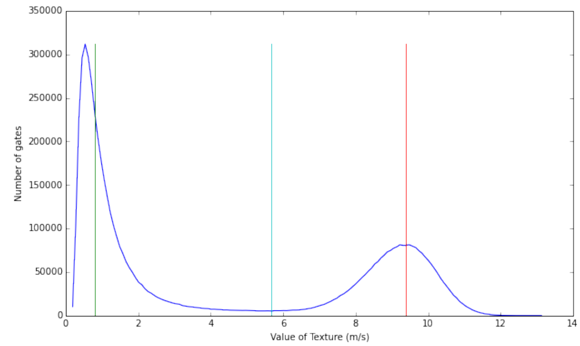

FIG. 4: Histogram of texture values from the volume shown in fig 3a. The left hand peak corresponds to significant returns, the right hand to noise. The black and red lines are the peak center guess by a wavelet based technique. The green line is the minimum value between the two peaks.

b. *Fuzzy logic based identification of scatterers at gate*

As previously discussed the aim of this step is to identify the dominant scatterer at each gate to aid in decision making upchain. Work has been done using fuzzy logic for precipitation determination before (see, for example Gourley et al. (2007)). However since ARM is not doing

3. Challeges

The data u

4. Future work

The climatology and varianc

Acknowledgments. Scott G
Patricia

References

Al-Sakka, H., A.-A. Boumahmoud, B. Fradon, S. J. Frasier, and P. Tabary, 2013: A New Fuzzy Logic Hydrometeor Classification Scheme Applied to the French X-, C-, and S-Band Polarimetric Radars. *Journal of Applied Meteorology and Climatology*, **52 (10)**, 2328–2344, doi:10.1175/JAMC-D-12-0236.1, URL http://journals.ametsoc.org/doi/abs/10.1175/JAMC-D-12-0236.1.

Dolan, B., and S. A. Rutledge, 2009: A Theory-Based Hydrometeor Identification Algorithm for X-Band Polarimetric Radars. *Journal of Atmospheric and Oceanic Technology*, **26 (10)**, 2071–2088, doi:10.1175/2009JTECHA1208.1, URL http://journals.ametsoc.org/doi/abs/10.1175/2009JTECHA1208.1.

Du, P., W. A. Kibbe, and S. M. Lin, 2006: Improved peak detection in mass spectrum by incorporating continuous wavelet transform-based pattern matching. *Bioinformatics*, **22 (17)**, 2059–2065, doi:10.1093/bioinformatics/btl355, URL http://bioinformatics.oxfordjournals.org/content/22/17/2059.abstract, http://bioinformatics.oxfordjournals.org/content/22/17/2059.full.pdf+html.

TABLE 1: Wide single-column table in a twocolumn document.

Class	Tex (m/s)	ρ_{HV}	NCP	Temperature (C)	height (km)	SNR (dB)
melting	[0, 0, 4, 6], 1.5	[0.6, 0.65, 0.9, 0.96], 3.5	[0.4, 0.5, 1, 1], 0	[0, 0.5, 6, 7], 1	[0, 0, 25, 25], 0	[8, 10, 1000, 1000], 0
multi trip	[5, 6, 130, 130], 5	[0.5, 0.7, 1, 1], 0	[0, 0, 0.5, 0.6], 0	[-100, -100, 100, 100], 0	[0, 0, 5, 8], 0	[15, 20, 1000, 1000], 1
rain	[0, 0, 4, 6], 1	[0.97, 0.98, 1, 1],1	[0.4, 0.5, 1, 1], 1	[2, 5, 100, 100], 2	[0, 0, 5, 6], 0]	[8, 10, 1000, 1000], 1
snow	[0, 0, 4, 6], 1	[0.65, 0.9, 1, 1],1	[0.4, 0.5, 1, 1], 1	[-100, -100, 0.5, 4], 2	[0, 0, 25, 25], 0	[8, 10, 1000, 1000], 1

Gourley, J. J., P. Tabary, and J. Parent du Chatelet, 2007: A Fuzzy Logic Algorithm for the Separation of Precipitating from Nonprecipitating Echoes Using Polarimetric Radar Observations. *Journal of Atmospheric and Oceanic Technology*, **24 (8)**, 1439–1451, doi:10.1175/JTECH2035.1, URL http://journals.ametsoc.org/doi/abs/10.1175/JTECH2035.1.

Heistermann, M., and Coauthors, 2014: The Emergence of Open Source Software for the Weather Radar Community. *Bull. Amer. Meteor. Soc.*, doi:10.1175/BAMS-D-13-00240.1, URL http://journals.ametsoc.org/doi/abs/10.1175/BAMS-D-13-00240.1.

James, C. N., and R. A. Houze, 2001: A Real-Time Four-Dimensional Doppler Dealiasing Scheme. *Journal of Atmospheric and Oceanic Technology*, **18 (10)**, 1674–1683, doi:10.1175/1520-0426(2001)018⟨1674:ARTFDD⟩2.0.CO;2, URL http://journals.ametsoc.org/doi/abs/10.1175/1520-0426(2001)018%3C1674%3AARTFDD%3E2.0.CO%3B2.

Jensen, M. P., and Coauthors, 2015: The Midlatitude Continental Convective Clouds Experiment (MC3e). *Bulletin of the American Meteorological Society*, doi:10.1175/BAMS-D-14-00228.1, URL http://dx.doi.org/10.1175/BAMS-D-14-00228.1.

Jones, E., T. Oliphant, P. Peterson, and Coauthors, 2001–: SciPy: Open source scientific tools for Python. URL http://www.scipy.org/, [Online; accessed 2016-03-02].

Kollias, P., and Coauthors, 2013: Scanning ARM Cloud Radars. Part II: Data Quality Control and Processing. *Journal of Atmospheric and Oceanic Technology*, **31 (3)**, 583–598, doi:10.1175/JTECH-D-13-00045.1, URL http://dx.doi.org/10.1175/JTECH-D-13-00045.1.

Mather, J. H., and J. W. Voyles, 2012: The Arm Climate Research Facility: A Review of Structure and Capabilities. *Bull. Amer. Meteor. Soc.*, **94 (3)**, 377–392, doi:10.1175/BAMS-D-11-00218.1, URL http://journals.ametsoc.org/doi/abs/10.1175/BAMS-D-11-00218.1.

Wen, G., A. Protat, P. T. May, X. Wang, and W. Moran, 2015: A Cluster-Based Method for Hydrometeor Classification Using Polarimetric Variables. Part I: Interpretation and Analysis. *Journal of Atmospheric and Oceanic Technology*, **32 (7)**, 1320–1340, doi:10.1175/JTECH-D-13-00178.1, URL http://dx.doi.org/10.1175/JTECH-D-13-00178.1.

Wikipedia, 2016: Directional statistics — wikipedia, the free encyclopedia. URL https://en.wikipedia.org/w/index.php?title=Directional_statistics&oldid=705952853, [Online; accessed 1-March-2016].